Biocatalysis

DOI: 10.1002/ange.201405016

Artificial Multienzyme Supramolecular Device: Highly Ordered Self-Assembly of Oligomeric Enzymes In Vitro and In Vivo**

Xin Gao, Shuai Yang, Chengcheng Zhao, Yuhong Ren, and Dongzhi Wei**

Abstract: *A strategy for scaffold-free self-assembly of multiple oligomeric enzymes was developed by exploiting enzyme oligomerization and protein–protein interaction properties, and was tested both in vitro and in vivo. Octameric leucine dehydrogenase and dimeric formate dehydrogenase were fused to a PDZ (PSD95/Dlg1/zo-1) domain and its ligand, respectively. The fusion proteins self-assembled into extended supramolecular interaction networks. Scanning-electron and atomic-force microscopy showed that the assemblies assumed two-dimensional layer-like structures. A fluorescence complementation assay indicated that the assemblies were localized to the poles of cells. Moreover, both in vitro and in vivo assemblies showed higher NAD(H) recycling efficiency and structural stability than did unassembled structures when applied to a coenzyme recycling system. This work provides a novel method for developing artificial multienzyme supramolecular devices and for compartmentalizing metabolic enzyme cascades in living cells.*

The construction of multiprotein supramolecular systems which self-assemble in predetermined ways is of broad interest owing to its potential applications in synthetic biology, nanotechnology,[1] and multienzyme biocatalysis.[2] Multienzymatic pathways in living systems are often segregated into microcompartments or organized as clusters.[3] This spatial ordering leads to more stable structures and facilitates substrate channeling between enzymes, thus resulting in increased yields from reactions.[4] Many artificial multienzyme assembly strategies exist, including enzyme fusion, scaffold-mediated enzyme colocalization, and enzyme polymerization induced by small molecules.[5,6]

Many known multienzyme cascades involve oligomeric enzymes, however, most available methods are difficult to adapt to their assembly, especially for enzymes with more than two subunits. The simplest way to construct a self-assembling complex is by enzyme fusion, which often results in the inclusion of inactive bodies or decreased enzymatic activity.[4,7] Scaffold-mediated methods may fail since each enzyme can be tethered by several scaffolds, while each scaffold might link multiple enzymes,[7] thus producing large, unstable, and disordered complexes. The random crosslinking between oligomers and scaffolds can also lead to steric hindrance between enzymes in a cascade, thereby weakening the effect of substrate channeling. Thus, better methods for promoting the self-assembly of multiple oligomeric enzymes are needed.

Construction of supramolecular assemblies using oligomer-to-multimer strategies, such as enzyme nanorings,[8] has been attempted, but most approaches have focused on the assembly of a single oligomeric enzyme in vitro. In this study, a strategy for the scaffold-free self-assembly of multiple oligomeric enzymes was demonstrated in vitro and in vivo by combining the enzyme property of homologous oligomerization and the heterogeneous high-affinity interaction between a protein domain and ligand.

Efficient regeneration of costly cofactors, which are essential for large-scale biotransformation using NAD(P)H-dependent oxidoreductases, represents a significant challenge in biosynthesis.[9] An effective strategy for facilitating cofactor regeneration in situ is to spatially bring together those oxidoreductases with the cofactor-regenerating dehydrogenases in a highly controlled manner.[10] However, a regeneration system which can self-assemble has not been developed thus far. Therefore, octameric leucine dehydrogenase (LDH) from *Bacillus subtilis* BEST7613 and dimeric formate dehydrogenase (FDH) from *Lodderomyces elongisporus* NRRL YB-4239, which constitute an NAD(H) recycling system for the production of L-*tert*-leucine,[11] were selected as a technologically relevant model for scaffold-free self-assembly of multiple oligomeric enzymes.

The strategy for the self-assembly of octameric LDH and dimeric FDH in vitro and in vivo is outlined in Figure 1. The PDZ (PSD95/Dlg1/zo-1) domain and corresponding ligand (PDZlig) from metazoan cells[6] were selected for the LDH and FDH interaction interface. The PDZ domain and PDZlig were fused to the C-termini of LDH and FDH, thus yielding LDH-PDZdomain (LPd) and FDH-PDZlig (FPl), respectively (Figure S1 B,C in the Supporting Information). To ensure complete accessibility of the PDZ domain and to prevent interactions between adjacent PDZ domains, a 5 nm rigid α-helical ER/K motif[12] was used to link the LDH subunit to the PDZ domain. It was predicted that after homologous oligomerization, FPls would connect LPds to form multienzyme supramolecular devices (LPd-FPl MESDs) when the two molecules were mixed in vitro or co-expressed in vivo.

[*] Dr. X. Gao, S. Yang, C. Zhao, Prof. Y. Ren, Prof. D. Wei
State Key Laboratory of Bioreactor Engineering
East China University of Science and Technology
Shanghai 200237, China
E-mail: yhren@ecust.edu.cn
dzhwei@ecust.edu.cn

[**] This work was funded by the National Special Fund for the State Key Laboratory of Bioreactor Engineering (2060204), the National Natural Science Foundation of China (No. 21076079), the National major science and technology projects of China (No. 2012ZX09304009), and the Fundamental Research Funds for the Central Universities of China.

Supporting information for this article is available on the WWW under http://dx.doi.org/10.1002/anie.201405016.

 © 2014 Wiley-VCH Verlag GmbH & Co. KGaA, Weinheim

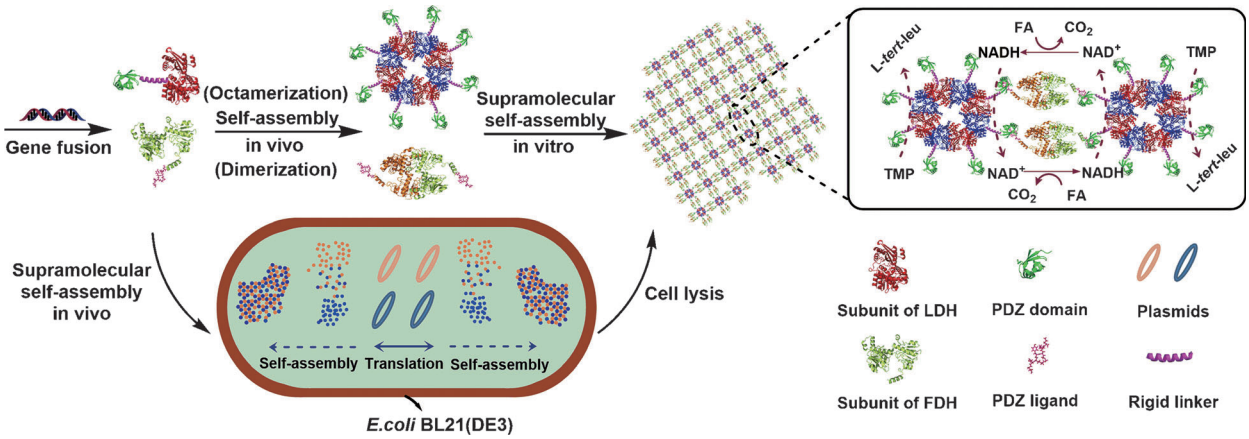

Figure 1. Strategy for the in vitro and in vivo self-assembly of octameric LDH and dimeric FDH. The scheme at the top right shows the putative reaction mechanism for the conversion of trimethylpyruvic acid (TMP) into L-*tert*-leucine catalyzed by assembled LDH and FDH. FA = ammonium formate.

The in vitro self-assembly system was constructed by expressing LPd and FPl in *Escherichia coli* BL21 (DE3) and purifying the proteins by nickel-chelating affinity chromatography. Both LPd and FPl were expressed in soluble form and retained almost all of the specific activity of the respective unfused proteins (see Figure S2), thus indicating that protein structures were not appreciably compromised by the fusion. The self-assembly was triggered by the mixture of purified FPl and LPd. The sodium dodecyl sulfate polyacrylamide gel electrophoresis (SDS-PAGE) analysis and dynamic light scattering (DLS) measurements (see Figure S3 A,B) showed that most of the FPls and LPds would be converted into LPd-FPl MESDs when the molar ratio of [FPl subunit] to [LPd subunit] was 1:1. Given this interaction,[13] the conversion of the assembly was almost unchanged when the ratio was greater or less than 1:1 (see Figure S4). The hydrodynamic diameter of protein in the mixture increased rapidly over time, and the bulk solution gradually changed from a clear to a white, turbid solution in 20 minutes (Figure 2 A b). The kinetics of the supramolecular assembly were determined by DLS measurements (Figure 2 B).

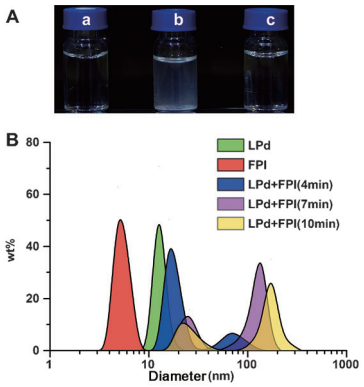

Figure 2. A) The solution states of pure LPd (a), the mixture of LPd and FPl at 20 min after mixing (b), and pure FPl (c) are shown. B) Dynamic light scattering analysis of the hydrodynamic diameter of pure LPd, pure FPl, and the mixture of LPd and FPl (LPd + FPl) at 4, 7, and 10 min after mixing ([FPl subunit]/[LPd subunit] = 1:1, 5 μM).

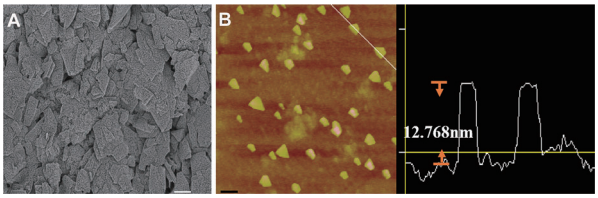

Figure 3. Structures of LPd and FPl self-assembled in vitro. Representative images from A) field-emission scanning electron and B) tapping-mode atomic-force microscopy. Results from the height assay are shown to the right; nanolayers had a height of approximately 12.8 nm. Scale bar = 200 nm. Samples were prepared at 20 min after mixing LPd and FPl ([FPl subunit]/[LPd subunit] = 1:1, 5 μM).

The morphology and structure of LPd-FPl MESDs were visualized by field-emission scanning electron and tapping-mode atomic-force microscopy. Images acquired by the former method showed LPd-FPl MESDs as highly ordered two-dimensional layer-like structures with diameters ranging from 100 to greater than 500 nm (Figure 3 A). A similar structure was observed by atomic-force microscopy, which revealed that the nanolayers were about 12.8 nm in height (Figure 3 B), which is in agreement with the value of 13 nm for naturally occurring LDH. The size of LPd-FPl MESDs was increased with increasing protein concentration from 1 to 5 μM (see Figures S3 C and S4). These results confirmed LPd-FPl MESD formation in vitro and showed that the interaction between dimeric FPl and octameric LPd molecules could be used to drive the growth of a supramolecular interaction network along a single plane.

To examine the effect of self-assembly on coenzyme regeneration efficiency, the biosynthesis of L-*tert*-leucine was catalyzed by LPd-FPl MESDs, with equal amounts of unassembled LDH and FDH used as a control. The reactions were performed at different NAD^+ concentrations for 1 hour, and the corresponding conversion ratios are summarized in Figure 4 A. Although the LPd-FPl MESDs exhibited only slightly higher NAD(H) recycling efficiency than unassembled LDH and FDH at high NAD^+ concentration (more than

© 2014 Wiley-VCH Verlag GmbH & Co. KGaA, Weinheim

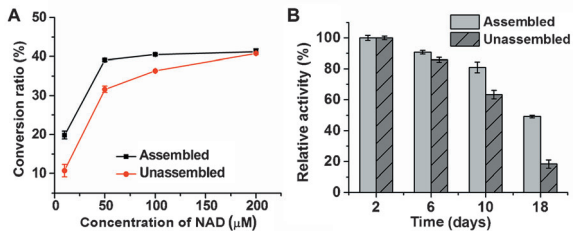

Figure 4. A) The conversion ratio for the first hour of L-*tert*-leucine-synthetized reactions catalyzed by LPd-FPl MESDs (5 μM) formed in vitro (assembled; black line) or by equal amounts of unassembled LDH and FDH (unassembled; red line) at various NAD^+ concentrations. B) Storage stability of LPd-FPl MESDs formed in vitro (assembled; solid bars) or unassembled LDH and FDH (unassembled; hatched bars). Data represent the mean ± standard deviation of three measurements. Initial activity was defined as 100%.

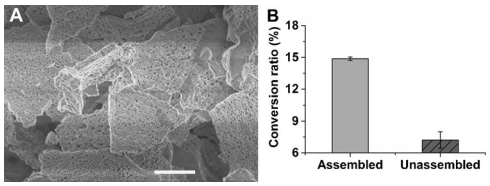

Figure 5. A) Image acquired by field-emission scanning electron microscopy of LPd and FPl self-assembled in vivo. Scale bar = 2 μm. B) The conversion ratio for the first hour of L-*tert*-leucine-synthesized reactions catalyzed by whole cells with self-assembled LPd and FPl (assembled) or with unassembled LDH and FDH (unassembled). Data represent the mean ± standard deviation of three measurements.

100 μM), the cofactor-recycling frequency (TOF) of the LPd-FPl MESDs was increased from 516 h^{-1} to 1007 h^{-1} at 10 μM of NAD^+ (see Table S1), and the conversion ratio for the first hour of the reaction was also increased by approximately twofold (Figure 4A). The saturated conversion of the reaction occurred at 50 μM of NAD^+ for the LPd-FPl MESDs and at 200 μM of NAD^+ for unassembled LDH and FDH because of NAD(H) saturation. In this case, the LPd-FPl MESDs and the unassembled LDH and FDH reached the maximum conversion ability of LPd and LDH (see Figure S2C), respectively. Furthermore, compared to unassembled LDH and FDH, the final conversion ratio was increased and the reaction time was significantly shortened for the LPd-FPl MESDs at low NAD^+ concentrations (see Figure S6). These results suggest that transfer channeling for NAD(H) occurred between LPd and FPl in LPd-FPl MESDs at a low concentration of NAD^+ (10 μM),[4] that is, when one NADH was transformed into NAD^+ by LPd for the synthesis of L-*tert*-leucine, the NAD^+ was immediately transferred to the adjacent FPl for NADH regeneration and vice versa, thus resulting in higher cofactor recycling efficiency.

The stability of multienzyme assemblies is a key factor for their widespread application in synthetic biology and biocatalysis or for their use as biosensors. The stability of LPd-FPl MESDs was thus evaluated by various assays. Compared to unassembled LDH and FDH, LPd-FPl MESDs had higher thermal stability, broader pH tolerance (see Figure S7), and higher storage stability: 50% of the initial activity of LPd-FPl MESDs was retained after storage at 4°C for 18 days, and was about threefold higher than that observed for unassembled LDH and FDH (Figure 4B). The improvement in structural stability could have been a result of the formation of precise supramolecular structures which restricted conformational changes in LPd and FPl during storage or exposure to different pH and temperature conditions.[14]

In vivo self-assembly was tested by co-expressing LPd and FPl in *E. coli* BL21 (DE3) and evaluating enzyme activity. FPl was present in both the precipitate and supernatant of the cell lysates, but LPd was confined almost exclusively to the precipitate (see Figure S8B). When used for L-*tert*-leucine biosynthesis, the precipitate had a conversion ratio of 80% after a 5 h reaction while the supernatant had negligible activity (see Figure S8C), thus suggesting that the LPd and FPl were assembled into largely insoluble LPd-FPl MESDs. This assembly was confirmed by field-emission scanning electron microscopy, which revealed micron-sized, layer-like structures in lysed cells which had a similar shape as but were larger than the LPd-FPl MESDs formed in vitro (Figure 5A).

The biosynthesis of L-*tert*-leucine by whole cells was used as a measure for the in vivo NAD(H) recycling efficiency of LPd-FPl MESDs. Cells expressing LPd-FPl MESDs had a twofold higher conversion ratio than whole cells co-expressing unassembled LDH and FDH (Figure 5B). This conversion could have been caused by the occurrence of NAD(H) transfer channeling as observed for LPd-FPl MESDs in vitro.

Fluorescence complementation experiments were performed to detect the formation of supramolecular assemblies in vivo and determine their subcellular compartmentalization. A red fluorescent protein (mCherry), divided into two parts (mN159 and mC160),[15] was fused to the C-terminus of LPd or the site between FDH and PDZlig in FPl, thus yielding LPd-mN159 (Lm) and FDH-mC160-PDZlig (FmP), respectively (see Figure S1D,E). Little fluorescence was detected when mN159 was co-expressed with mC160 (see Figure S9), however, the fluorescence increased markedly when Lm and FmP were coexpressed (Figure 6A,B), and signal localization indicated that the LPd-FPl MESDs were confined to the poles of cells. A possible reason for this is that the supramolecular assembly of LPd and FPl triggered the transport of protein aggregates to these compartments where they formed a large complex.[16]

To determine the conversion kinetics for in vivo assembly, the fluorescence intensity of cells co-expressing Lm and FmP was measured at various times after the addition of isopropyl β-D-1-thiogalactopyranoside (IPTG). The fluorescence intensity increased sharply after 9 hours (Figure 6C), possibly because the protein concentration in the cells (see Figure S8A) had increased to a level which produced a high conversion rate for assembly. Moreover, the value reached a maximum after 21 hours, thus suggesting that the assembly was completed. Based on the time taken for assembly and catalytic efficiency (Figure 6D), the optimal length of time for IPTG-induced expression was determined to be 18 hours.

A method was developed for the self-assembly of multiple oligomeric enzymes which was successfully applied to in vitro and in vivo systems. The LPd-FPl MESDs generated by this

 © 2014 Wiley-VCH Verlag GmbH & Co. KGaA, Weinheim

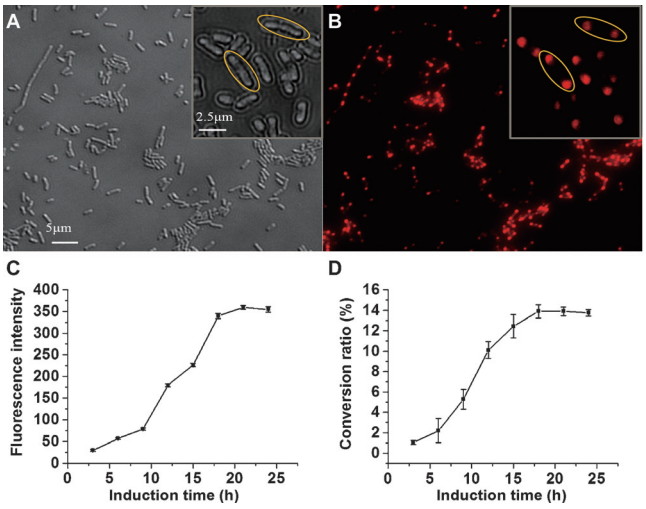

Figure 6. LPd and FPl self-assembled in vivo and visualized using an mCherry-based fluorescence complementation system. Cells were imaged by A) differential interference contrast and B) epifluorescence. LPd-FPl MESDs localized to the poles of cells (yellow circles). C) Fluorescence intensity of cells (1 mg) co-expressing Lm and FmP at indicated times after IPTG addition. D) The conversion ratio for the first hour of L-*tert*-leucine-synthesized reactions catalyzed by whole cells (10 mg mL^{-1}) expressing LPd-FPl MESDs at indicated times after IPTG addition. Data represent the mean ± standard deviation of three measurements.

method had a highly ordered, two-dimensional layer-like structure and demonstrated a mechanism of NAD(H) transfer channeling which resulted in improved NAD(H) recycling efficiency compared to that of unassembled LDH and FDH. LPd-FPl MESD compartmentalization at cell poles was demonstrated by fluorescence complementation. These results indicate that this supramolecular self-assembly strategy is a powerful tool for multienzyme biocatalysis which increases yields from reactions by substrate channeling, and provides a novel approach for compartmentalizing metabolic enzyme cascades in living cells.

Received: May 6, 2014
Revised: June 19, 2014
Published online: October 15, 2014

Keywords: biocatalysis · enzyme catalysis · oligomerization · self-assembly · supramolecular chemistry

[1] a) F. Baneyx, J. F. Matthaei, *Curr. Opin. Biotechnol.* **2014**, *28*, 39–45; b) G. Bellapadrona, M. Elbaum, *Angew. Chem. Int. Ed.* **2014**, *53*, 1534–1537; *Angew. Chem.* **2014**, *126*, 1560–1563; c) J. D. Brodin, J. R. Carr, P. A. Sontz, F. A. Tezcan, *Proc. Natl. Acad. Sci. USA* **2014**, *111*, 2897–2902.
[2] S. Howorka, *Curr. Opin. Biotechnol.* **2011**, *22*, 485–491.
[3] C. J. Delebecque, A. B. Lindner, P. A. Silver, F. A. Aldaye, *Science* **2011**, *333*, 470–474.
[4] C. You, S. Myung, Y. H. P. Zhang, *Angew. Chem. Int. Ed.* **2012**, *51*, 8787–8790; *Angew. Chem.* **2012**, *124*, 8917–8920.
[5] a) S. Schoffelen, J. C. van Hest, *Soft Matter* **2012**, *8*, 1736–1746; b) N. P. King, Y.-T. Lai, *Curr. Opin. Struct. Biol.* **2013**, *23*, 632–638; c) Y.-T. Lai, K.-L. Tsai, M. R. Sawaya, F. J. Asturias, T. O. Yeates, *J. Am. Chem. Soc.* **2013**, *135*, 7738–7743.
[6] J. E. Dueber, G. C. Wu, G. R. Malmirchegini, T. S. Moon, C. J. Petzold, A. V. Ullal, K. L. Prather, J. D. Keasling, *Nat. Biotechnol.* **2009**, *27*, 753–759.
[7] H. Lee, W. C. DeLoache, J. E. Dueber, *Metab. Eng.* **2012**, *14*, 242–251.
[8] Y. Bai, Q. Luo, W. Zhang, L. Miao, J. Xu, H. Li, J. Liu, *J. Am. Chem. Soc.* **2013**, *135*, 10966–10969.
[9] J. H. Schrittwieser, J. Sattler, V. Resch, F. G. Mutti, W. Kroutil, *Curr. Opin. Chem. Biol.* **2011**, *15*, 249–256.
[10] J. Rocha-Martín, B. d. L. Rivas, R. Munoz, J. M. Guisán, F. López-Gallego, *ChemCatChem* **2012**, *4*, 1279–1288.
[11] U. Kragl, D. Vasic-Racki, C. Wandrey, *Bioprocess Eng.* **1996**, *14*, 291–297.
[12] S. Sivaramakrishnan, J. Sung, M. Ali, S. Doniach, H. Flyvbjerg, J. Spudich, *Biophys. J.* **2009**, *97*, 2993–2999.
[13] B. Z. Harris, B. J. Hillier, W. A. Lim, *Biochemistry* **2001**, *40*, 5921–5930.
[14] C. Hou, J. Li, L. Zhao, W. Zhang, Q. Luo, Z. Dong, J. Xu, J. Liu, *Angew. Chem. Int. Ed.* **2013**, *52*, 5590–5593; *Angew. Chem.* **2013**, *125*, 5700–5703.
[15] J.-Y. Fan, Z.-Q. Cui, H.-P. Wei, Z.-P. Zhang, Y.-F. Zhou, Y.-P. Wang, X.-E. Zhang, *Biochem. Biophys. Res. Commun.* **2008**, *367*, 47–53.
[16] A. Rokney, M. Shagan, M. Kessel, Y. Smith, I. Rosenshine, A. B. Oppenheim, *J. Mol. Biol.* **2009**, *392*, 589–601.

© 2014 Wiley-VCH Verlag GmbH & Co. KGaA, Weinheim